PCCP

Accepted Manuscript

ROYAL SOCIETY OF CHEMISTRY

www.rsc.org/pccp

Cite this: DOI: 10.1039/c0xx00000x

www.rsc.org/xxxxxx

ARTICLE TYPE

Probing framework-guest interactions in phenylene-bridged periodic mesoporous organosilica using spin-probe EPR

Feng Lin,[a,b] Xiangyan Meng,[a] Myrjam Mertens,[c] Pegie Cool,[a] and Sabine Van Doorslaer[*,b]

Received (in XXX, XXX) Xth XXXXXXXXX 20XX, Accepted Xth XXXXXXXXX 20XX

DOI: 10.1039/b000000x

The pore walls of phenylene-bridged periodic mesoporous organosilicas (B-PMOs) can be crystal-like or amorphous depending on the synthesis conditions. Here, spin-probe electron paramagnetic resonance (EPR) is used to monitor the adsorption of nitroxide radicals on three types of B-PMO with varying pore size and wall characteristics. Nitroxide radicals with varying polarity are chosen as probes to mimic guest molecules with different properties. The study shows that the B-PMO materials with amorphous walls allow an overall better adsorption of the spin probes than the one with crystalline walls, independent of the nature of the spin probe. The effect of hydration of the guest-host system on the mobility of the spin probe molecule depends more on the nature of the spin probe than on the B-PMO material. Comparison of the spin-probe adsorption on B-PMOs and ethylene-bridged PMO materials shows the sensitivity of the mobility of the guest molecule on the nature of the organic group.

Introduction

Periodic mesoporous organosilicas (PMOs)[1-4] form a new class of porous inorganic-organic hybrid materials with highly ordered mesoporous structures, and with the organic groups as an integral part of the inorganic-oxide framework. In contrast to the organically functionalized mesoporous silicas, which are usually obtained either by a grafting approach or alternatively by co-condensation,[5,6] the inorganic and organic moieties are covalently linked to each other and homogeneously distributed in the framewall of PMOs. This has extended the research of mesoporous materials from "chemistry of the void space" to "chemistry of the walls". Due to the presence of the organic groups within the framewall, PMOs have a tunable surface hydrophobicity/hydrophilicity, unique mechanical and hydrothermal stability,[7] and adsorption capacity, leading to materials with promising potential in catalysis, metal scavenging and controlled drug release. Of particular interest are PMOs with phenylene-bridged units as they can exhibit both ordered mesopores and molecular-scale order of the phenylene groups within the pore walls. This molecular periodicity can enable structural orientation of guest molecules enclosed in the pores, which in turn may improve the selectivity and activity in catalytic applications.[8] Moreover, the phenylene groups in the pore wall allow post-modification such as sulfonation[9,10] and amination[11], which is very important for catalytic applications. In fact, all potential catalytic applications of mesoporous materials involve insertion and/or immobilization of molecules in the pores of the materials and the activity of the materials is dramatically influenced by the nature of their surface. Knowledge of the surface properties of PMO materials is thus of paramount relevance for the practical application.

Onida *et al*. investigated the surface properties of phenylene-bridged PMOs by means of combined IR and computational studies.[12-14] The authors showed that the aromatic rings in the framewall make the isolated silanol species of the phenylene-bridged PMOs less acidic than in pure silica materials. They also found that the phenylene-bridged PMOs with amorphous walls consist of slightly more acidic silanols compared to phenylene-bridged PMOs with crystal-like walls.[15] A study of the adsorption of CO on phenylene-bridged PMOs revealed a bifunctional nature of the surface, with the CO-framework interactions with CO interacting with both the aromatic rings and the silanols.[12] By comparison of the hydrogen adsorption capacity of different PMOs and pure silica material, Okubo *et al*. found that PMOs with π electrons can adsorb more hydrogen molecules per unit area, and have higher isosteric heat of hydrogen adsorption than PMOs that have no π electrons.[16] Iodine adsorption experiments revealed that there are more exposed phenylene sites able to interact with iodine on the surface of PMOs with amorphous walls than in PMOs with crystalline walls.[17]

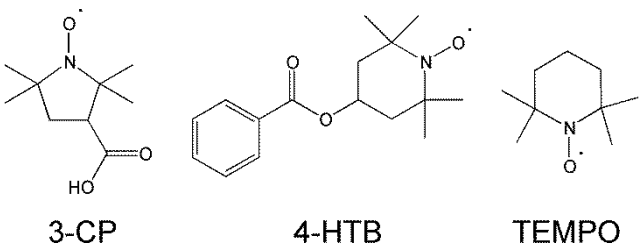

Scheme 1 Chemical formula of the spin probes used in this work: 3-Carboxy-Proxyl (3-CP), 4-Hydroxy-TEMPO Benzoate (4-HTB) amd 2,2,6,6-Tetramethylpiperidine 1-oxyl (TEMPO).

Cite this: DOI: 10.1039/c0xx00000x

www.rsc.org/xxxxxx

ARTICLE TYPE

Among the different techniques available for material characterization, spin-probe electron paramagnetic resonance (EPR) has revealed itself to be an excellent tool to analyze the surface properties of porous materials.[18] By analyzing the EPR spectra of paramagnetic spin probes, mostly nitroxide radicals, that can interact with the surface sites of the porous materials, information about the structure, accessibility, surface polarity and surface charge can be obtained. Spin-probe EPR has shown to reveal relevant information about zeolites[19,20], mesoporous silica materials[21-26] and PMO materials[27,28].

In the present paper, spin-probe EPR will be used to investigate the surface properties of phenylene-bridged PMOs with different molecular-scale ordering and different pore structures. To this end, three different kinds of spin probes (Scheme 1) are adsorbed on the PMO materials. The selected spin probes present different polarities and hence interact differently with the pore surface. Complemented by X-ray powder diffraction, FT-IR spectroscopy and N_2 adsorption-desorption experiments, the spin-probe EPR analyses give an insight into pore accessibility and surface polarity.

Materials and methods

Materials

All starting materials were used as purchased without further purification: 1,4-bis(triethoxysilyl)-benzene (BTEB, 96% Sigma-Aldrich), cetyltrimethylammonium bromide (CTMABr, 99% Sigma-Aldrich), Pluronic P123 triblock copolymer (EO_{20}-PO_{70}-EO_{20}, Sigma-Aldrich), Brij-76 ($C_n(EO)_{10}$, Sigma-Aldrich), HCl (37% Acros Organic), NaOH (98.5% Acros Organic), $CHCl_3$ (99.9% Acros Organic). The spin probe 3-Carboxy Proxyl (3-CP), 4-Hydroxy-TEMPO Benzoate (4HTB) and TEMPO were purchased from Sigma-Aldrich.

Synthesis of phenylene-bridged PMO materials

Three different recipes reported by Inagaki *et al.*[8,29] and Onida and co-workers[17] were employed to prepare phenylene-bridged PMO materials with different pore size and wall characteristics. Hereafter the resulting samples will be referred to as B-PMO-A, B-PMO-B and B-PMO-C, respectively.

B-PMO-A was synthesized with the following composition: 1.0 BTEB : 1.11 CTMABr : 4.15 NaOH : 652 H_2O. In a typical synthesis of B-PMO-A[8], 3.05 g CTMABr was dispersed into 90 mL of a 0.33 M NaOH solution. Subsequently, 3 mL of BTEB was drop-wise added. The whole mixture is then placed in an ultrasonic bath for 20 minutes. Afterwards, the substance was stirred for 20 hours at room temperature and successively transferred to an autoclave for a hydrothermal treatment of 24 hours at 373 K.

B-PMO-B was synthesized with the following composition: 1.0 BTEB: 0.336 Brij-76 : 30.1 HCl: 1782 H_2O. In a typical synthesis of B-PMO-B[29], 1.26 g Brij-76 was dissolved in a mixture of 159 g water and 13.1 ml 37% HCl solution. 2 ml BTEB was added under vigorous stirring at room temperature. The solution was subsequently stirred at room temperature for 20 hours, and then transferred to an autoclave for a hydrothermal treatment of 24 hours at 423K.

B-PMO-C was synthesized with the following composition: 1.0 BTEB: 0.034 P123 : 0.48 HCl: 400 H_2O. In a typical synthesis of B-PMO-C[17]: 1.04 g P123 was dissolved in 35.5 g water, and added to 2.5 ml 1M HCl solution. 2 ml BTEB was added into the above solution and then stirred at 273K for 1 hour. The mixture was then heated at 313 K for 20 hours with stirring, and followed by aging in an autoclave at 373K for another 24 hours.

In all cases, the white precipitate obtained was filtered, washed thoroughly with deionised water, and dried at room temperature. Surfactant template removal was accomplished by two solvent extraction cycles with ethanol containing HCl at 333 K.

Spin-probe adsorption procedure

Prior to the spin-probe adsorption experiment, the template-free samples were dehydrated under high vacuum for 24 hours at 100ºC. 300 mg of dehydrated PMOs was stirred for 10 h in 5ml of a chloroform solution of the spin probe (5 x 10^{-4} M). Afterwards, the solid was filtered and washed two times with pure chloroform to remove the spin probes adsorbed on the external surface. Then, the samples were dried at room temperature under dry air conditions.

Characterization methods

N_2 adsorption–desorption isotherms were obtained at liquid N_2 temperature (77 K) using a Quantachrome Quadrasorb-SI automated gas adsorption system. Prior to adsorption, the samples were outgassed under high vacuum for 16 hours at 100 ºC. The specific surface area was calculated using the Brunauer–Emmet–Teller (BET) method, between a relative pressure of 0.05 and 0.35. The pore size distributions were deduced from the desorption branches of the isotherms using the Barrett–Joyner–Halenda (BJH) method. The total pore volumes were calculated from the amount of N_2 vapour adsorbed at a relative pressure of 0.95. The micropore area and volume were calculated by the *t*-plot method using experimental points at a relative pressure of $P/P_0 = 0.10–0.20$.

X-ray diffraction (XRD) measurements were recorded on a Pananalytical X'PERT PRO MPD diffractometer with filtered CuKα-radiation. The measurements were performed in the 2θ mode using a bracket sample holder with a scanning speed of 0.04°/4 s in continuous mode.

Thermogravimetric analysis (TGA/DTG) results were recorded on a Mettler Toledo TGA/ SDTA851. The analyses were performed in an oxygen atmosphere, whereby the samples were heated from 30 °C to 700 °C with a heating rate of 5 °C/min.

Cite this: DOI: 10.1039/c0xx00000x

www.rsc.org/xxxxxx

ARTICLE TYPE

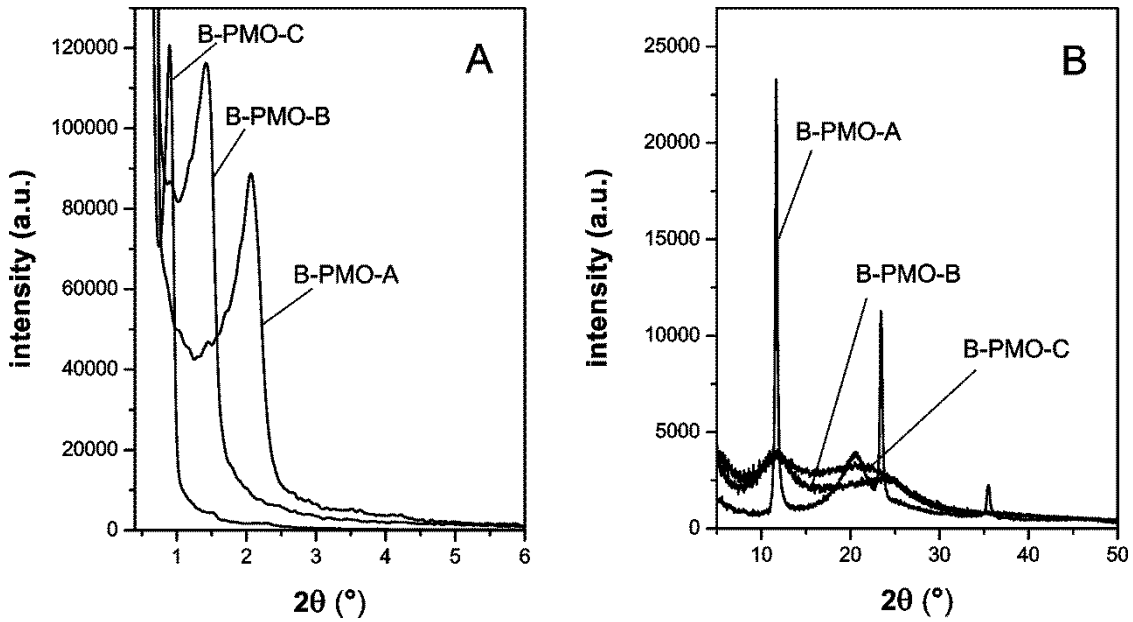

Fig. 1 (A) Small-angle and (B) wide-angle powder XRD patterns of the three types of phenylene-bridged PMOs under study.

FT-IR (DRIFT) measurements were recorded on a Nicolet 20 DXB Fourier Transform IR spectrometer equipped with a DTGS detector. Pure KBr was measured as a reference for the background. The samples were diluted with KBr (2% sample, 98% KBr). The resolution was set to 4 cm^{-1} and 200 scans were averaged. All measurements were performed under a flow of dry air.

X-band continuous-wave (CW)-EPR measurements were performed on a Bruker ESP 300E instrument, equipped with a liquid helium cryostat (Oxford Inc.), working at a microwave (mw) frequency of about 9.5 GHz. A microwave power of 1 mW, a modulation frequency of 100 kHz and a modulation amplitude of 0.5 mT were applied. The number of spins was determined via double integration of the EPR spectra. For this, the integration values were compared to those of standards of chloroform solutions of nitroxide spin probes with known concentrations and volumes. All measured PMO samples were weighed carefully to allow calculation of the spin concentration (mol spins/g PMO).

Results and discussion

Structural characterization

The small angle XRD patterns of the three types of phenylene-bridged PMOs under study are shown in Figure 1A. All samples exhibit an intense reflection peak in the 2θ range of 0.5-3º, which can be assigned to the d(100) inter-planar spacing of a two-dimensional hexagonal symmetry structure, akin to MCM-41 or SBA-15 mesophases. The d(100) peak position is different for the three samples. This can be associated with the different pore size of the materials (d-values are reported in Table 1).

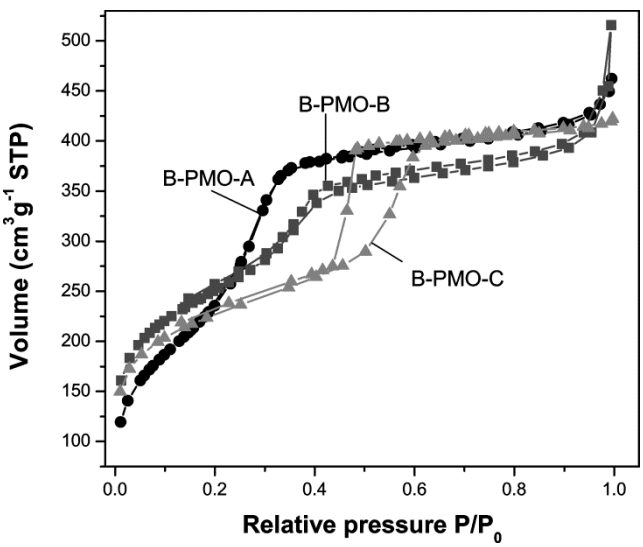

Fig. 2 N_2 adsorption-desorption isotherms of the three types of phenylene-bridged PMOs under study

In the wide angle region (Figure 1B), three additional peaks at 2θ-values 12º, 23º, and 35º appear for B-PMO-A, which is synthesized with CTAB as surfactant under basic hydrolytic conditions. These peaks can be attributed to the regular arrangement of the phenylene groups within the pore wall (crystal–like wall structure)[8]. Although for B-PMO-B and B-PMO-C a distinct peak at 2θ =12º can still be observed, its intensity is much lower than that of B-PMO-A, indicating the poor order of the phenylene groups. This is in agreement with previous reports which revealed that the highly molecular-scale

order of the phenylene groups is difficult to achieve under acidic conditions.[29-31] Furthermore a broad reflection peak at 2θ=20° can be observed for all three samples, which can be ascribed to the amorphous nature of atomic arrangements of Si and O in the framework. This peak is commonly observed in mesoporous silica materials.[32]

The nitrogen adsorption-desorption isotherms of the three samples are shown in Figure 2 and their corresponding structural properties are listed in Table 1. All of the isotherms are of type IV with a sharp increase in the adsorption volume at a relative pressure of 0.20-0.65 due to the capillary condensation, indicating a uniform mesoporous structure. For B-PMO-A and B-PMO-B, the isotherms do not exhibit a distinct hysteresis loop, the pore sizes obtained by the BJH model are 2.5 nm and 2.8 nm, respectively, and no micropores were identified using the *t*-plot method. In contrast, the isotherm of B-PMO-C shows a clear H1-type hysteresis loop at high relative pressure, which is characteristic of large-pore mesoporous materials. Furthermore, a slight microporosity is observed in this material, which is due to the penetration of the polyethylene-oxide chains of the triblock copolymer template (Pluronic P123) into the hydrophilic pore walls during synthesis.[29,33]

Table 1 Structural parameters of the three types of phenylene-bridged PMOs investigated in this study.

Sample	B-PMO-A	B-PMO-B	B-PMO-C
d value (nm)	4.29	6.22	9.82
Wall thickness (nm)	2.45	4.38	6.64
Surface area (m^2g^{-1})	851	880	805
Pore size (nm)	2.5	2.8	4.7
Pore volume (cm^3g^{-1})	0.695	0.703	0.649
Micropore volume (cm^3g^{-1})	-	-	0.162

A thermogravimetrical analysis was performed under air flow for the three types of phenylene-bridged PMO materials (TGA curves, see ESI). As shown in the DTG thermogram in Figure 3, only two weight loss peaks can be observed. The weight loss below 120 °C is due to the thermodesorption of physisorbed water or ethanol, and the weight loss between 400-700 °C is assigned to the decomposition of the phenylene moieties within the framework. No obvious weight loss due to the surfactant was observed, indicating the complete removal of the template through solvent extraction. It is noticed that, compared to B-PMO-A, the second weight-loss peak (decomposition of the phenylene groups), has shifted to lower temperatures for B-PMO-B and B-PMO-C. The phenylene-bridged PMOs display relative thermal stabilities in the order B-PMO-A > B-PMO-B > B-PMO-C. In fact, the decomposition of the phenylene moieties in B-PMO-A occurs over the range 500-700 °C, while for B-PMO-B, the decomposition begins at 450 °C. Interestingly, the framework decomposition happens already at 400°C for B-PMO-C, although this PMO possesses the most thick pore wall among these three samples (Table 1). This observation is very interesting, since it contrasts the finding for inorganic silica materials, where the thick pore walls of SBA-15 are responsible for the higher hydrothermal stability compared to the other mesoporous silica with thin pore walls like MCM-41 or MCM-48.[34,35] Most likely, the lower decomposition temperature of B-PMO-C is due to the presence of micropores within the pore wall, which indeed increase the opportunity for the organic groups to react with O_2 during the thermogravimetrical analysis. Furthermore, it seems that the orientation of the aromatic rings also plays a role in the thermal stability of the phenylene-bridged PMOs, which is evidenced by the lower decomposition temperature of B-PMO-B with thicker pore walls compared to that of B-PMO-A with thin pore walls.

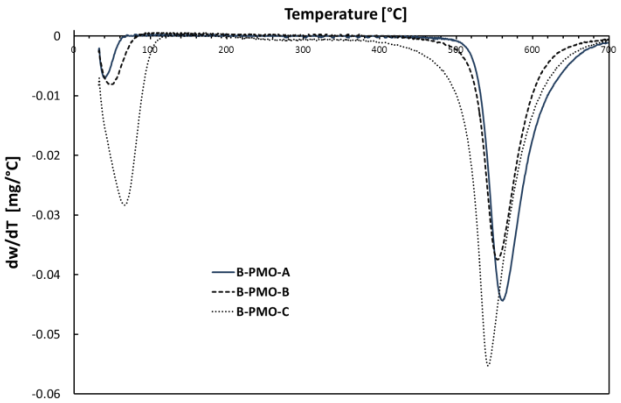

Fig. 3 DTG measurements of three types of phenylene-bridged PMOs under study

Adsorption of spin probes on phenylene-bridged PMOs

As mentioned earlier, all potential applications of mesoporous materials involve insertion and/or immobilization of molecules in the pores of the material. Spin-probe EPR has been shown to be a unique tool to monitor the incorporation of molecules in the pores of such systems.[18] The spin probes can be considered to be mimics of the active molecules that one would like to insert in the materials. The three spin probes used in this study (Scheme 1) are sufficiently smaller than the pore sizes of the phenylene-bridged PMO materials, so that pore-size effects can be excluded as a limiting factor for the probe uptake and adsorption.

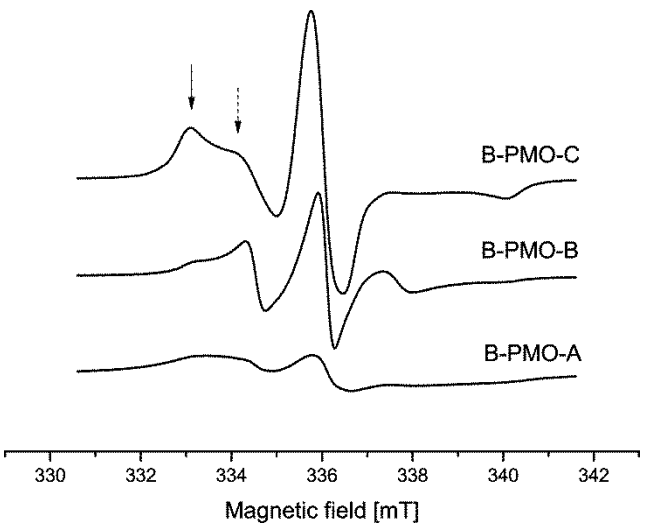

Fig. 4 Room-temperature CW-EPR spectra of 3-CP adsorbed on the different dehydrated phenylene-bridged PMO materials under study. The spectra are shown such that they reflect the relative intensity of the three spectra. The arrows indicate the marker peaks for the slow-motion (solid arrow) and fast-motion (dashed) phase of the spin label.

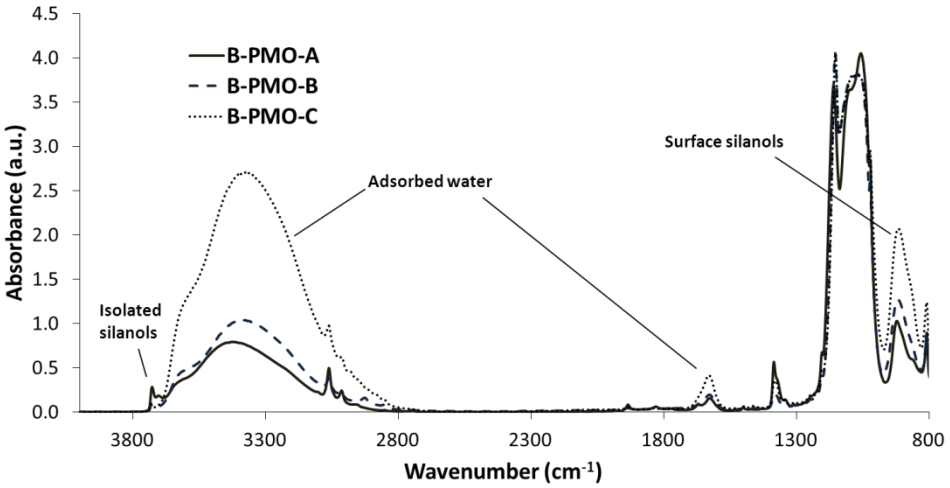

Fig. 5 FT-IR spectra of the template-free phenylene-bridged PMO materials under study. No special dehydration treatment was applied.

Due to its polar head (-COOH group), 3-CP is very easy to dissolve in water. 3-CP is amphiphilic, able to interact both with its polar or non-polar side with the surface of PMO materials.[27] Adsorption of the polar head of 3-CP onto the PMO surface occurs through hydrogen bonding with the surface silanols, quite similar to the interaction reported for other polar probes.[36] The phenylene group in the 4-HTB structure renders the molecule quite hydrophobic. The adsorption of 4-HTB on the PMO surface will thus be mainly via π-π stacking interactions between the aromatic rings of 4-HTB and PMO surface. In contrast, no special interaction is expected for the TEMPO molecules, other than those present for all spin probes because of the nitroxide unit (van der Waals interactions and possible hydrogen bonding to the nitroxide group). Therefore, the TEMPO molecules are expected to bind weaker to the PMOs surface than the other two spin probes.

Table 2 Spin concentrations (10^{-6} mol spins/g PMO) of the spin probes in different phenylene-bridged PMO materials. Experimental error is 10%.

	B-PMO-A	B-PMO-B	B-PMO-C
3-CP	3.8	4.7	6.2
4-HTB	0.4	1.7	1.9
TEMPO	1.5	2.0	3.2

Figure 4 shows the EPR spectra of 3-CP adsorbed on the three types of phenylene-bridged PMOs. The EPR intensity increases in the following sequence: B-PMO-A ≤ B-PMO-B < B-PMO-C (Table 2). The EPR spectral intensity of 3-CP adsorbed on B-PMO-C is considerably higher than that of 3-CP adsorbed on the other two materials, which indicates that a larger amount of 3-CP molecules remains in the pores of B-PMO-C. The most likely adsorption sites for 3-CP molecules are the silanols on the surface of the material (stabilization through hydrogen bonding).

In order to probe the possible surface differences, FT-IR experiments were performed on the three types of phenylene-bridged PMOs (template-free without further dehydration treatment) (Figure 5; see ESI for detailed assignment). The broad band between 3100~3700 cm^{-1} can be assigned to the adsorbed water (or water of crystallization) and O-H vibrations, while the band at 920 cm^{-1} shows the presence of residual silanols, (ν(Si-OH), stretching vibrations[37]). Compared with the B-PMO-A and B-PMO-B, B-PMO-C contains much more silanols, which will result in more possible adsorption sites for 3-CP on B-PMO-C than on the other two materials. The larger amount of surface water in B-PMO-C illustrates the aptness of the material to take up polar molecules.

The differences in the EPR spectral features of 3-CP adsorbed on the different phenylene-bridges PMOs (Figure 4) also reflect the differences in motion of the spin probes in the pores of the materials. Although EPR spectra recorded at a large variety of microwave frequencies are needed to be able to correctly determine the motional parameters of spin probes,[38] the spectra recorded at a single microwave frequency can be used to obtain qualitative motional information. Simulations of the EPR spectra of 3-CP adsorbed on dehydrated B-PMO-C and B-PMO-B (see ESI) reveal that the spectra cannot be reproduced assuming a single motion type for the spin probe. In both materials, the EPR spectra are the result of at least two sets of the probes with different motional behaviour, a faster and slower tumbling phase (ESI). Both these phases are slower for the 3-CP molecules adsorbed on B-PMO-C than for 3-CP on B-PMO-B. This can already be qualitatively evaluated from Figure 4. The lower-field peak indicated with the solid arrow in Figure 4 is a marker for the slow motion of the molecule, while a sharp peak in the area indicated by the dashed arrow reflects the presence of a faster rotating probe. The EPR-spectrum of 3-CP adsorbed on B-PMO-A shows much broader EPR lines typical of spin-spin interactions

(Figure 4 and ESI for enlargement of spectrum). This indicates that although the overall spin concentration is lower than in the B-PMO-B and B-PMO-C cases (Table 2), the local concentration of 3-CP is higher (clustering of 3-CP indicating pore blocking). The different pore structure of the materials will be an important factor determining the motion of the spin probes. B-PMO-C, which is synthesized with P123 as the surfactant, exhibits a unique dual pore system formed by hexagonally arranged cylindrical mesopores with micropores within the walls.[39-41] Some of the 3-CP molecules might be trapped in the micropores of B-PMO-C, and thus exhibit a slower motion within the reduced space, agreeing with the fact that the slowest 3-CP motion is found for the B-PMO-C case rather than for the B-PMO-B material. The trapping of 3-CP in the micropores is likely, since the spin probe TEMPO, which has a similar molecular size as 3-CP, has already been reported to be able to enter the faujasite cavities of zeolites X and Y, with a concomitant low mobility[20]. This confinement of the probe in the micropores of B-PMO-C may also explain the higher adsorption of 3-CP on this material (less leaching). Nevertheless, the existence of micropores in the B-PMO-C material cannot be the only factor that plays a role in determining the 3-CP motion. In order to unravel this further, adsorption experiments with 4-HTB and TEMPO were performed (Figure 6,7).

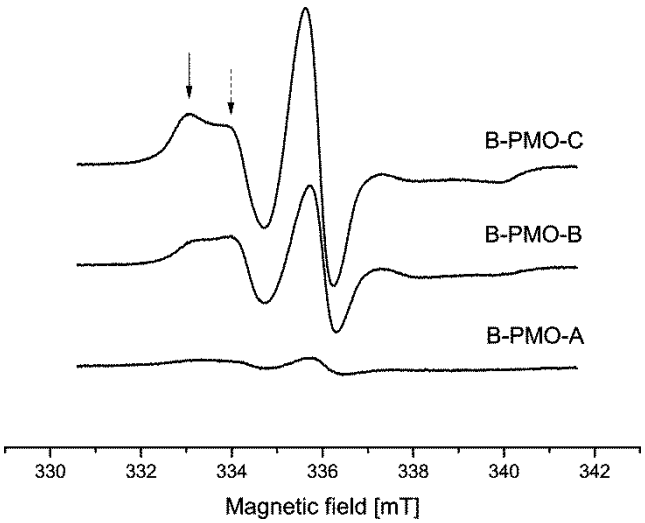

Fig. 6 Room-temperature CW-EPR spectra of 4-HTB adsorbed on the different dehydrated phenylene-bridged PMO materials under study. The spectra are shown such that they reflect the relative intensity of the three spectra. The arrows indicate the marker peaks for the slow-motion (solid) and fast-motion (dashed) phase of the spin label.

The EPR intensities of 4-HTB adsorbed on the three types of phenylene-bridged PMOs show a similar sequence as observed for 3-CP: B-PMO-A<B-PMO-B≤B-PMO-C, but now with a marked lower adsorption of 4-HTB on B-PMO-A than on the other PMOs. Again, the linewidth of the EPR spectrum of 4-HTB on B-PMO-A is very broad suggesting high local concentration of the spin probes and possible local clustering or blocking of pores. The EPR spectra of 4-HTB of B-PMO-B and B-PMO-C reflect complex motions on the spin probes, with a qualitatively lower mobility of the spin probe in B-PMO-C (more pronounced low-field peak indicated by the solid arrow in Figure 6). The reduced mobility may be (partially) due to the presence of micropores in B-PMO-C. Since B-PMO-A and B-PMO-B lack the micropores and have comparable specific surface areas and mesopore size (Table 1), and have comparable surface silanol amounts (Figure 5), the lower adsorption of 4-HTB on B-PMO-A must be due to other surface properties. Considering that the adsorption sites of 4-HTB on the phenylene-bridged PMOs are most likely the aromatic rings, this result suggests a lower accessibility of the aromatic rings in B-PMO-A. The main difference between B-PMO-A and the other two materials is the molecular-scale periodicity in the framework. B-PMO-A, synthesized with CTAB as a surfactant under basic hydrolytic conditions, has crystal-like pore walls[8] (Figure 1B). It contains molecularly ordered phenylene groups which are lying perpendicular to the pore surface.[8] In contrast, the wide-angle XRD results of B-PMO-B and B-PMO-C (Figure 1B) show that the periodicity of the phenylene groups in the pore wall is very poor for these materials. The poor order of the phenylene groups implies variations in the torsion angles of phenylene groups relative to the surface. Hence some phenylene groups will expose the phenylene ring to the surface and thus give rise to more accessible adsorption sites for the 4-HTB molecules. Our findings confirm the results of the iodine adsorption experiment on crystal-like and amorphous-wall B-PMOs[17]. The iodine, which preferentially interacts with the phenylene groups, is found to be most strongly adsorbing on the surface of the phenylene-bridged PMOs with amorphous walls.

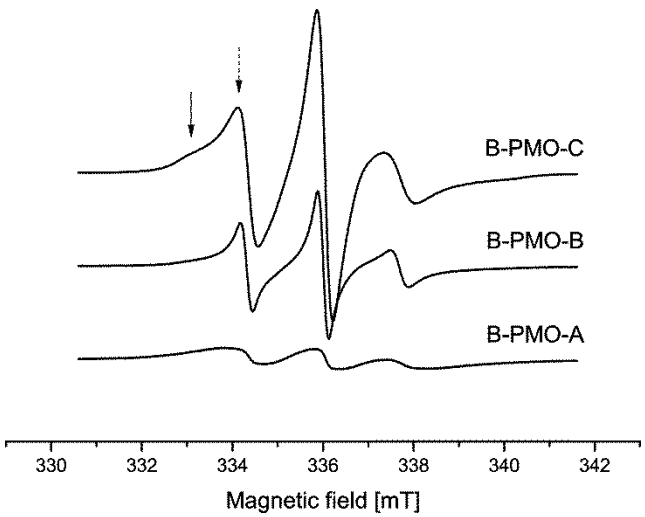

Fig. 7 Room-temperature CW-EPR spectra of TEMPO adsorbed on the different dehydrated phenylene-bridged PMO materials under study. The spectra are shown such that they reflect the relative intensity of the three spectra. The arrows indicate the marker peaks for the slow-motion (solid) and fast-motion (dashed) phase of the spin label.

The EPR spectra of TEMPO adsorbed on the three types of phenylene-bridged PMOs under study reveal a higher mobility of the TEMPO molecule than of 3-CP and 4-HTB (compare Figure 7 with Figures 4 and 6: for each PMO material the sharpest fast-motion marker (dashed arrow) is found for TEMPO). It is interesting to notice that the intensities of the EPR spectra again follow the sequence: B-PMO-A<B-PMO-B<B-PMO-C.

Cite this: DOI: 10.1039/c0xx00000x

www.rsc.org/xxxxxx

ARTICLE TYPE

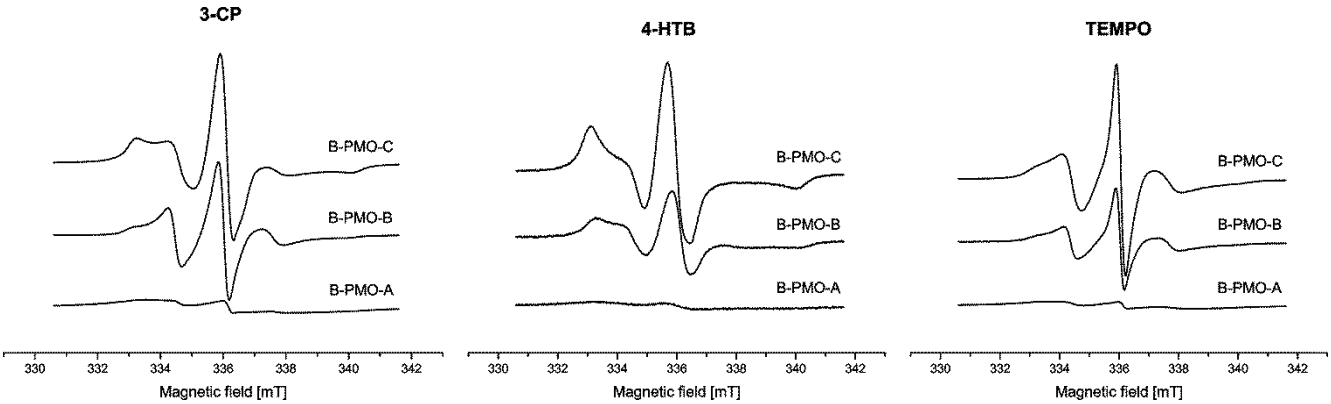

Fig. 8 Room-temperature CW-EPR spectra of 3-CP, 4-HTB and TEMPO adsorbed on the different phenylene-bridged PMO materials under study after rehydration of the samples in air. For each spin probe the spectra are depicted such that they reflect the relative intensity of the three spectra.

It is known that the permanent dipole moments of the nitroxide units interact with the electrostatic field of the surface and the unit can be stabilized by hydrogen bonds.[20] This interaction influences the adsorption and the mobility of the spin probes in the material. As mentioned, the main structural difference between B-PMO-A and B-PMO-B or B-PMO-C is the different orientation of the aromatic rings in the PMO wall. Because of the perpendicular orientation of the aromatic rings to the pore surface in B-PMO-A, only few π-electron clouds will be exposed to the surface. In B-PMO-B or B-PMO-C, the random orientation of the aromatic rings will allow van der Waals interactions between the TEMPO molecule and the pore surface. Therefore, the TEMPO molecules will prefer adsorption to the amorphous walls of B-PMO-B and B-PMO-C. Furthermore, a fraction of the TEMPO molecules is immobilized in B-PMO-C (Figure 7, solid arrow). Again, this may be attributed to spin-probe molecules trapped in the micropores of this material.

In view of the above results, we can now understand the adsorption behaviour of the spin probes on the PMO materials. The adsorption experiments of 4-HTB and TEMPO showed that, apart from the surface silanols, the molecular order of the aromatic rings in the PMO walls also plays an important role in effecting the surface properties. As mentioned, van der Waals binding exists for all spin probes with a nitroxide unit and this unit may form hydrogen bonds. The driving force for the adsorption of 3-CP on the surface of the phenylene-bridged PMOs will thus result from a combination of H-bonding of the acid group and van der Waals binding/hydrogen bonding of the nitroxide unit. Similarly, π-π stacking between the phenylene units of 4-HTB and the PMO materials will compete with the binding interactions of the nitroxide. This explains the existence of different spin probe populations with different motional behaviour even in the PMO materials that exhibit only mesopores (existence of slow and fast phases, see ESI). Both B-PMO-A and B-PMO-B have a comparable (low) amount of surface silanol groups making the orientation of the aromatic rings in the material an important factor for the adsorption of the spin probes. Indeed, the overall lower adsorption amount of the spin probes on B-PMO-A can be attributed to the perpendicular orientation of the aromatic rings to the pore surface in B-PMO-A.

Finally, the EPR line broadening at low temperature depends on the dipole-dipole interaction between the electron spins.[42] As a measure for the broadening, the relative intensities of the central (d) and outer (d_1) lines of the EPR signals of the nitroxide radicals can be employed (ESI). The d_1/d value[43] is inversely related to the average inter-molecular distance of the spin probes adsorbed on the surface of PMO materials. Hence, it can, to some extent, reflect the dispersion conditions of the spin probes. From Table S2 (ESI), it can be seen that the d_1/d values are always the largest for the spin probes adsorbed on B-PMO-A, indicating the highest local concentration of the spin probes. This confirms the earlier observed line-broadening at room temperature. Together with the observation that the overall EPR intensity is always the lowest for spin-probe adsorption on B-PMO-A (Figures 4, 6 and 7), this indicates that the spin probes aggregate at the entrance of the pores, blocking the access to channels.

Furthermore, the fact that the EPR line width (d_1/d) is varying for all samples implies that the dipolar interaction influences the spectra and that the inter-spin distances are thus below 3 nm in all cases. This is far less than the inter-spin distance that is estimated from the experimental spin concentration and surface area assuming a random distribution law (ESI) (distances well above 7 nm), showing that the spin probes are not homogeneously distributed in the materials. This implies that the spin probes are not able to penetrate fully the phenylene-bridged PMO materials. In the B-PMO-A samples, the penetration degree is the lowest. The current experiments thus show that the crystalline walls of B-PMO-A can be disadvantageous for insertion of molecules in the pores and thus may in some cases hamper applications.

Effect of surface water on the behaviour of the adsorbed spin probes

Water molecules can easily adsorb at silanol sites. Our spin-probe EPR study on the surface properties of ethylene-bridged PMOs has shown that surface water and surface polarity also play a decisive role in probe insertion and immobilization[28]. Since many applications of nanoporous materials imply contact with water vapour, it is important to study the effect of surface water on the behaviour of the spin probes in the B-PMO materials. For this purpose, the phenylene-bridged PMOs adsorbed with spin probes were rehydrated by exposure of the materials to (moist) air for several hours, and measured with EPR at room temperature (Figure 8). Comparison with the EPR spectra in Figures 4, 6 and 7 shows that the mobility of the spin probes changes after rehydration (visible in the change of the shape of the EPR feature; see ESI for overlay of spectra before and after rehydration). Contrary to what may be expected, rehydration (*i.e.* increase of solvent in the pores) does not lead in all cases to an increased mobility of the spin probes. In fact, lower molecular motion is observed for 4-HTB and TEMPO, while no or a small increase in the mobility is observed for 3-CP. Due to its high hydrophobicity 4-HTB hardly dissolves in water. Rehydration of the PMO material will strengthen the interaction between the molecule and the phenylene units of the PMO material leading to a decrease in the molecular mobility. On the contrary, TEMPO is a water-soluble probe and one would expect an increased mobility. TEMPO molecules can, however, be coupled to the interfacial water via a hydrogen bond which is approximately 30% stronger than the H_2O-H_2O hydrogen bond.[44] This particular feature of TEMPO-water interaction may slow down the movement of the TEMPO molecules and may explain the surprising change in the molecules' motion. Possibly, the hydrogen bonding of the nitroxide to the silanol units also plays a role, leading to a reduction of the tumbling of TEMPO because of the hydrophobic interactions, the hydrophilic NO group being inaccessible to water due to the solvent. The H-bonding between the silanol groups and the acidic end group and/or nitroxide group of 3-CP may also explain why no major increase in the mobility of the polar 3-CP is observed.

Effect of the nature of the organic group on the spin-probe mobility

It is clear that the nature of the organic group in the PMO wall will be very important in determining the PMO's properties. In this last part of the study, we compare the adsorption of the spin probes to B-PMO-B and an ethylene-bridged PMO (see ESI). The latter PMO was extensively studied by us in earlier work.[28] B-PMO-B was chosen because, just as the ethylene-bridged PMO, it lacks micropores and crystallinity of the wall. Both PMOs were dehydrated prior to probe adsorption. While TEMPO and 4-HTB exhibit a faster motion in the ethylene-bridged PMO when compared to B-PMO-B, the movement of 3-CP is reduced in the ethylene-bridged PMO (ESI). Owing to the phenylene units, the surface of phenylene-bridged PMOs is more hydrophobic than that of ethylene-bridged PMOs. The strong hydrophobic environment makes the surface of the phenylene-bridged PMOs exhibit a higher affinity for the hydrophobic 4-HTB molecule and hence reduces its mobility. The van der Waals interactions between TEMPO and the PMO wall will be stronger in the B-PMO-B case (because of the phenylene units), which may explain the somewhat reduced motion of TEMPO in this PMO. The increase of the motion of 3-CP in B-PMO-B may be due to its amphiphilic nature. 3-CP tends to stay at the interface region and adsorb with its polar or non-polar side depending on the polarity of the solvent (used to introduce the probe) versus the surface polarity. [27] A recent study showed that the mobility of the spin probe increases as the difference between the solvent and surface polarity decreases.[27] The larger mobility of 3-CP in B-PMO-B than in the ethylene-bridged PMO may thus reflect a surface polarity closer to that of chloroform in the former case.

Conclusions

Spin-probe EPR provides a simple way to probe the framework-guest interactions in phenylene-bridged PMOs with different molecular-scale ordering and different pore structures.

The adsorption of spin probes with varying polarity has revealed the bi-functional nature of the surface of phenylene-bridged PMOs, including both aromatic rings and silanols. It is found that the pore structure and the orientation of the aromatic rings within the framewall are very important in determining the thermal stability and surface properties of the phenylene-bridged PMOs. Generally, phenylene-bridged PMOs with amorphous walls allow an overall better adsorption of the spin probes than the one with crystalline walls, independent of the nature of the spin probe. Furthermore, spin probes can be trapped into the micropores of the material. In contrast, the effect of hydration of the guest-host system on the mobility of the spin-probe molecule depends more on the nature of the spin probe than on the type of phenylene-bridged PMO material. After rehydration, the mobility of 4-HTB and TEMPO molecules in phenylene-bridged PMOs decreases, while no effect or a slight increase of the molecular motion is observed for 3-CP. The comparison of the spin-probe adsorption on phenylene-bridged PMOs and ethylene-bridged PMO materials showed that the organic group in the PMO wall plays an important role in effecting the behaviour of the guest molecules on its surface.

Acknowledgments

The Erasmus Mundus CONNEC program is acknowledged for PhD funding of F.L. Furthermore, the authors acknowledge support by the GOA-BOF project 'Towards new approaches in bioelectrochemistry – Targeted immobilization of globins on porous materials', funded by the University of Antwerp.

Notes and references

[a] *Laboratory of Adsorption and Catalysis, Department of Chemistry, University of Antwerp, Universiteitsplein 1, B-2610, Wilrijk, Belgium. Fax: +32 3 2652374; Tel: : +32 3 2652355; E-mail: pegie.cool@uantwerpen.be*
[b] *BIMEF Laboratory, Department of Physics, University of Antwerp, Universiteitsplein 1, B-2610, Wilrijk, Belgium.; Fax: +32 3 2652470; Tel: +32 3 2652461; E-mail: sabine.vandoorslaer@uantwerpen.be*
[c] *Flemish Institute for Technological Research, VITO, Boerentang 200, B-2400,Mol, Belgium*

† Electronic Supplementary Information (ESI) available: (1) TGA analysis of phenylene-bridged PMO materials, (2) Additional analysis of FT-IR spectra of phenylene-bridged PMO materials, (3) EPR spectra of 3-CP in phenylene-bridged PMOs: spin-probe mobility analysis, (4) Evalution of the dipolar interaction between the spin probes adsorbed on the surface of B-PMOs, (5) Comparison of the EPR spectra before and after rehydration of the PMO materials, (6) Details of synthesis of ethylene-bridged PMO materials, (7) CW-EPR of spin-probe adsorption on ethylene-bridged PMO compared to B-PMO-B. See DOI: 10.1039/b000000x/

‡ Footnotes should appear here. These might include comments relevant to but not central to the matter under discussion, limited experimental and spectral data, and crystallographic data.

1 T. Asefa, M. J. MacLachlan, N. Coombs, and G. A. Ozin, *Nature*, 1999, **402**, 867.

2 S. Inagaki, S. Guan, Y. Fukushima, T. Ohsuna and O. Terasaki, *J. Am. Chem. Soc.*, 1999**, 121**, 9611.

3 F. Hoffmann, M. Cornelius, J. Morell and M. Froba, *Angew. Chem. Int. Edit.*, 2006**, 45**, 3216.

4 P. Van der Voort, D. Esquivel, E. De Canck, F. Goethals, I. Van Driessche, and F. J. Romero-Salguero, *Chem. Soc. Rev.*, 2013**, 42**, 3913.

5 K. Moller, and T. Bein, *Mesoporous Molecular Sieves* 1998**, 117**, 53.

6 A. Stein, B. J. Melde and R. C. Schroden, *Adv. Mater.*, 2000**, 12**, 1403.

7 M. C. Burleigh, M. A. Markowitz, S. Jayasundera, M. S. Spector, C. W. Thomas and B. P. Gaber, *J. Phys. Chem. B*, 2003**, 107**, 12628.

8 S. Inagaki, S. Guan, T. Ohsuna and O. Terasaki, *Nature*, 2002**, 416**, 304.

9 Q.H. Yang, M. P. Kapoor and S. Inagaki, *J. Am. Chem. Soc.*, 2002**, 124**, 9694.

10 Q.H. Yang, J. Liu, J. Yang, M. P. Kapoor, S. Inagaki and C. Li, *J. Catal.* 2004**, 228**, 265.

11 M. Ohashi, M.P. Kapoor and S. Inagaki, *Chem. Commun.* 2008, 841.

12 B. Camarota, P. Ugliengo, E. Garrone, C. O.Arean, M. R. Delgado, S. Inagaki and B. Onida, *J. Phys. Chem. C* 2008**, 112**, 19560.

13 B. Onida, B. Camarota, P. Ugliengo, Y, Goto, S. Inagaki and E. Garrone, *J. Phys. Chem. B* 2005**, 109**, 21732.

14 B. Onida, L. Borello, C. Busco, P. Ugliengo, Y. Goto, S. Inagaki and E. Garrone, *J. Phys. Chem. B* 2005**, 109**, 11961.

15 B. Camarota, B. Onida, Y. Goto, S. Inagaki and E. Garrone, *Langmuir*, 2007**, 23**, 13164.

16 M. Kubo, K. Ishiyama, A. Shimojima, and T. Okubo, *Microporous Mesoporous Mater.* 2012**, 147**, 194.

17 B. Camarota, Y. Goto, S. Inagaki, E. Garrone and B. Onida, *J. Phys. Chem. C*, 2009**, 113**, 20396.

18 S. Ruthstein, and D. Goldfarb, *Electron Paramagn. Reson*. 2008, **21**, 184.

19 D. C. Doetschman and G. D. Thomas, *Chem. Phys.*, 1998**, 228**, 103.

20 M. F. Ottaviani, M. Garciagaribay, and N. J. Turro, *Colloid Surface A*, 1993**, 72**, 321.

21 A. Moscatelli, A. Galarneau, F. Di Renzo, M. F. Ottaviani, *J. Phys. Chem. B*, 2004**, 108**, 18580.

22 M. Okazaki, S. Anandan, S. Seelan, M. Nishida, and K. Toriyama, *Langmuir*, 2007**, 23**, 1215.

23 M. Okazaki and K. Toriyama, *J. Phys. Chem. C*, 2007**, 111**, 9122.

24 J. Y. Zhang, Z. Luz, and D. Goldfarb, *J. Phys. Chem. B*, 1997, **101**, 7087.

25 J. Y. Zhang, Z. Luz, H. Zimmermann and D. Goldfarb, *J. Phys. Chem. B*, 2000, **104**, 279.

26 S. Ruthenstein, V. Frydman, S. Kababya, M. Landau and D. Goldfarb, *J. Phys. Chem. B*, 2003, **107**, 1739.

27 M. Wessig, M. Drescher and S. Polarz, *J. Phys. Chem. C*, 2013**, 117**, 2805.

28 L. Feng, M. Mertens, P. Cool and S. Van Doorslaer, *J. Phys. Chem. C*, 2013**, 117**, 22723.

29 Y. Goto and S. Inagaki, *Chem. Commun*., 2002, 2410.

30 W.H. Wang, W. Z. Zhou, and A. Sayari, *Chem. Mater*., 2003**, 15**, 4886.

31 M. P. Kapoor, N. Setoyama, Q. H. Yang, M. Ohashi, and S. Inagaki, *Langmuir*, 2005, **21**, 443.

32 H. Song, R. M. Rioux, J. D. Hoefelmeyer, R. Komor, K. Niesz, M. Grass, P. D. Yang, and G. A. Somorjai, *J. Am. Chem. Soc.*, 2006**, 128**, 3027.

33 V. Meynen, P. Cool, and E. F. Vansant, *Microporous Mesoporous Mater*., 2007, **104**, 26.

34 K. Cassiers, T. Linssen, M. Mathieu, M. Benjelloun, K. Schrijnemakers, P. Van Der Voort, P. Cool and E. F. Vansant, *Chem. Mater.*, 2002**, 14**, 2317.

35 D. Y. Zhao, Q. S. Huo, J. L. Feng and B. F. Chmelka, *J. Am. Chem. Soc.*, 1998**, 120**, 6024.

36 M. Okazaki, K. Toriyama, N. Sawaguchi and K. Oda, *Appl. Magn. Res*on., 2003, **23**, 435.

37 B. Schrader, *Infrared and Raman spectroscopy: methods and applications, VCH, Weinheim* 1995.

38 B. Dzikovsky, D. Tipikin, V. Livshits, K. Earle and J. Freed, *Chem. Phys. Phys. Chem*., 2009, **11**, 6676.

39 D. Y. Zhao, J. L. Feng, Q. S. Huo, N. Melosh, G. H. Fredrickson, B. F. Chmelka and G. D. Stucky, *Science* 1998**, 279**, 548.

40 K. Miyazawa and S. Inagaki, *Chem. Comm.* 2000, 2121.

41 A. Nossov, E. Haddad, F. Guenneau, A. Galarneau, F. Di Renzo, F. Fajula, and A. Gedeon, *J. Phys. Chem. B* 2003**, 107**, 12456.

42 S. S. Eaton and G. R. Eaton, in *Biological Magnetic Resonance 19*, ed. L. J. Berliner, S. S. Eaton and G. R. Eaton, Kluwer, New York, 2000, ch. 1, pp. 1-27.

43 Y. Kano, K. Kushimoto, K. Komaguchi, Y. Ooyama, I. Imae, J. Ohshita and Y. Harima, *Phys. Chem. Chem. Phys.* 2012**, 14**, 15988.

44 D. G. Wu, A. D. Malec, M. Head-Gordon, and M. Majda, *J. Am. Chem. Soc.*, 2005**, 127**, 4490.